Hindawi Publishing Corporation
International Journal of Rotating Machinery
Volume 2007, Article ID 29270, 10 pages
doi:10.1155/2007/29270

Research Article

Investigations on the Blade Vibration of a Radial Inflow Micro Gas Turbine Wheel

Shijie Guo

Element Technology Lab., Tokai Rubber Industries, Ltd., 1 Higashi 3-chome, Komaki-shi, Aichi-ken 485-8550, Japan

Received 7 September 2006; Accepted 3 February 2007

Recommended by Seung Jin Song

This paper demonstrates the investigations on the blade vibration of a radial inflow micro gas turbine wheel. Firstly, the dependence of Young's modulus on temperature was measured since it is a major concern in structure analysis. It is demonstrated that Young's modulus depends on temperature greatly and the dependence should be considered in vibration analysis, but the temperature gradient from the leading edge to the trailing edge of a blade can be ignored by applying the mean temperature. Secondly, turbine blades suffer many excitations during operation, such as pressure fluctuations (unsteady aerodynamic forces), torque fluctuations, and so forth. Meanwhile, they have many kinds of vibration modes, typical ones being blade-hub (disk) coupled modes and blade-shaft (torsional, longitudinal) coupled modes. Model experiments and FEM analysis were conducted to study the coupled vibrations and to identify the modes which are more likely to be excited. The results show that torque fluctuations and uniform pressure fluctuations are more likely to excite resonance of blade-shaft (torsional, longitudinal) coupled modes. Impact excitations and propagating pressure fluctuations are more likely to excite blade-hub (disk) coupled modes.

1. INTRODUCTION

With the increasing requirements for distributed power supply and cogeneration systems, much attention is being paid to micro gas turbines. As a result, the micro gas turbine business as well as related R&D have grown considerably in recent years [1, 2]. One of the key topics in the design of micro gas turbines is structure analysis for preventing bursting, creeping, fatigue, and problems such as contact with casing and performance decrease due to large deformation. Small gas turbines have long been used in industrial applications such as APUs (auxiliary power units) [3, 4]. However, APUs only operate for short durations, providing air for the cabin on the ground, and are only a back up system at the higher load cases to provide electrical power in case of a main engine generator failure. Micro gas turbines in distributed power supply or cogeneration systems are required to operate continuously at various loads and so design criteria for the two systems tend to be quite different. Furthermore, partial load efficiency can be improved by running at slower speeds thereby reducing the mass flow rate. Therefore, it is important to have a good understanding of blade vibration to define a blade geometry that can operate over a wide speed range. Configuration of the rotor of a micro gas turbine is similar to that of a turbocharger if we do not consider the generator/motor. But a micro gas turbine works at much higher temperature and heavier loads.

Since the turbine wheel is exposed to very high temperature during operation, the dependence of Young's modulus on temperature is a major concern in structural analysis. Many data have been published [5, 6] for typical high temperature metals. But almost all of them are the measurement data on ideal specimens. In this research, a real turbine wheel was investigated to understand not only the value of Young's modulus but also its anisotropy, scattering, and dependence on the cutting location. The results were compared with other published data [6]. The wheel was made by investment casting. Heat treatment and HIP (hot isotropic press) were conducted.

On the other hand, a turbine rotor consists of a turbine wheel, a compressor impeller, an iron core (generator/motor), and a shaft. It is well known that turbine blades suffer many excitations during operation, such as pressure fluctuations (unsteady aerodynamic forces), torque fluctuations, and so forth. Meanwhile, the blades have many different vibration modes. Typical ones are the blade-hub (disk)

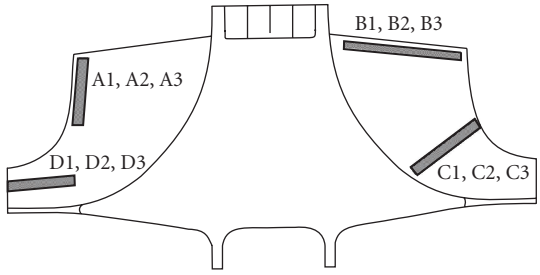

Figure 1: Locations of the specimens.

coupled modes (the blade bending modes coupled with the hub's nodal diameter vibration), the blade-shaft (torsional) coupled modes (the blade bending modes coupled with the shaft's torsional vibration), as well as the blade-shaft (longitudinal) coupled modes (the blade bending modes coupled with the shaft's longitudinal vibration). Kreuz-Ihli et al. [7] studied the pressure fluctuations acting on the blades of a radial inflow turbine wheel by using CFD (computational fluid dynamics) and analyzed the blade-hub (disk) coupled vibration by using FEM (finite element method). They stated that vibration of blade-hub (disk) coupled modes can be excited by pressure fluctuations. Iwaki et al. [8, 9] measured the blade vibration in a turbocharger during operation by strain gauges. Their results showed that blade resonance can be excited by pressure fluctuations of the higher harmonic components of the rotating frequency, and that damping ratios of the blade bending modes are very small. In this research, model experiments and FEM analysis were conducted to investigate the coupled vibrations and to reveal which modes, among all the modes mentioned above, are more likely to be excited under various excitations.

2. IDENTIFICATION ON YOUNG'S MODULUS AT HIGH TEMPERATURE

Young's modulus of the blades of a real radial inflow turbine wheel was investigated to understand its dependence on temperature, its scattering, and the possible existence of anisotropy. The wheel was made of M-Mar247. Heat treatment and HIP were conducted at 1185°C under 172 MPa for 4 hours, 1185°C for 2 hours, and 870°C for 20 hours. Specimens were cut out from different blades in different directions as shown in Figure 1: three specimens from three different blades along the tip (shroud) near the trailing edge (A1–A3), along the trailing edge (B1–B3), across the mid span (C1–C3), near the leading edge (D1–D3), respectively. A brief description about the identification on Young's modulus is provided as follows [10, 11]. A specimen was suspended in a furnace by thin ceramic threads so that it could vibrate without constraints. Ambient temperature near the heated specimen was measured using a thermocouple. A small steel ball was dropped onto the specimen to give it an impact excitation. The ringing sound emitted from the impacted specimen was measured by using a microphone. The signal from the microphone was analyzed using an FFT (fast Fourier transform) analyzer to obtain natural frequencies. Young's modulus was then estimated by an inverse calculation from the natural frequencies at a free-support boundary condition.

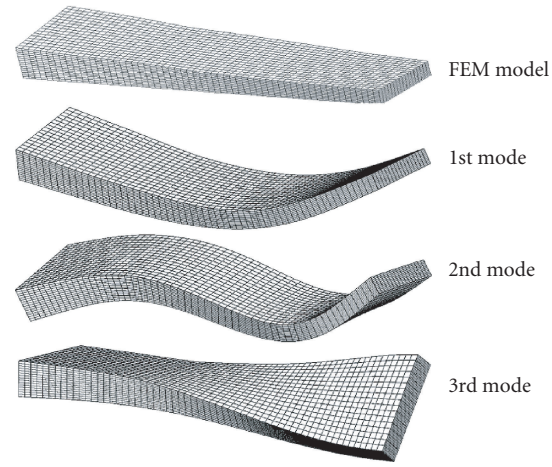

Figure 2: FEM model and vibration modes of specimen B1.

FEM, beam theory, as well as shell theory are usually used for the inverse calculation, depending on the geometry of the specimen. In this research, FEM was used considering that the specimens are curved and tapered. Figure 2 shows the FEM model and the vibration modes of specimen B1 as an example. The 1st mode and the 2nd mode are bending modes, the 3rd one is a torsional mode. There are two bending modes and one torsional mode within the three lowest modes for all the specimens. Only the two bending modes were used in the identification because the two modes are dominated by Young's modulus in the longitudinal direction of a specimen. Poisson's ratio has not much influence on the two bending modes, but has a relatively strong relation with the torsional mode. Since natural frequencies of the torsional mode were not measured accurately for some specimens, Poisson's ratio was not identified. Considering that it does not have much influence on the bending vibration, it was assumed to be 0.3 in the FEM analysis.

Measurements on natural frequencies of the specimens were conducted at room temperature, 200°C, 400°C, 600°C, 700°C, 800°C, 900°C, and 1000°C, respectively. Each specimen was heated in the furnace for one hour before the measurement at each temperature. Figure 3 gives the impact responses of specimen B1 at room temperature (21°C) and high temperature (900°C) as an example of the measurement results. Natural frequencies decrease as temperature increases. The identification results on Young's modulus from all the specimens are plotted in Figure 4, in which the shaded area is the scatter band from [6]. Figure 4 shows that Young's modulus decreases as temperature increases, but its scattering for different specimens is limited. Since the specimens were cut out from different blades in different directions, the limited scattering means that Young's modulus does not have much anisotropy and its dependence on the cutting location

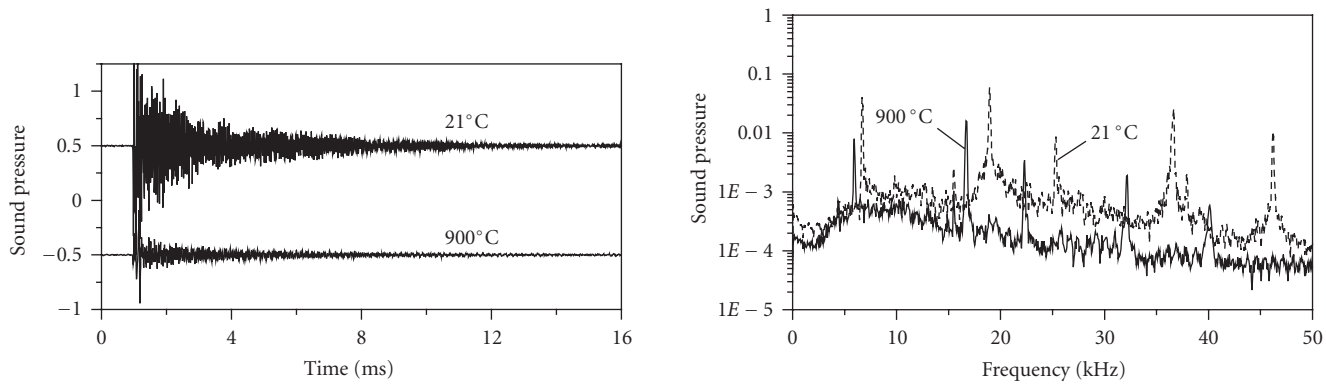

Figure 3: Time history and frequency spectra of the impact responses of specimen B1 at room temperature (21°C) and high temperature (900°C).

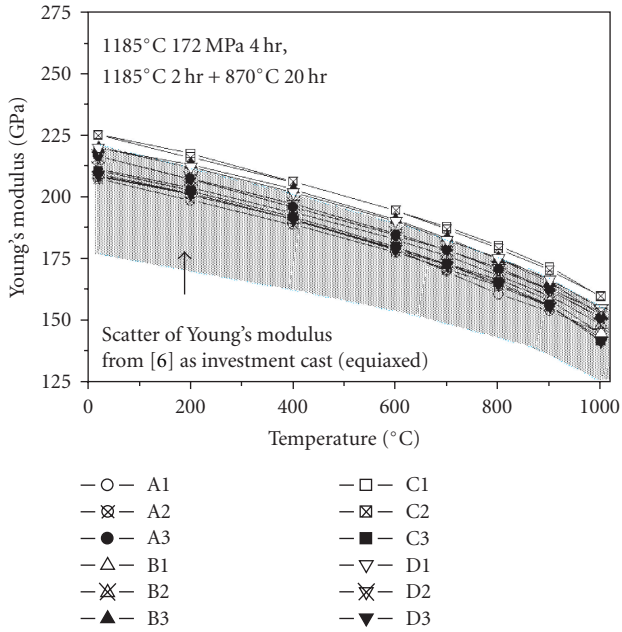

Figure 4: Young's modulus identified from the specimens cut out from different blades in different directions.

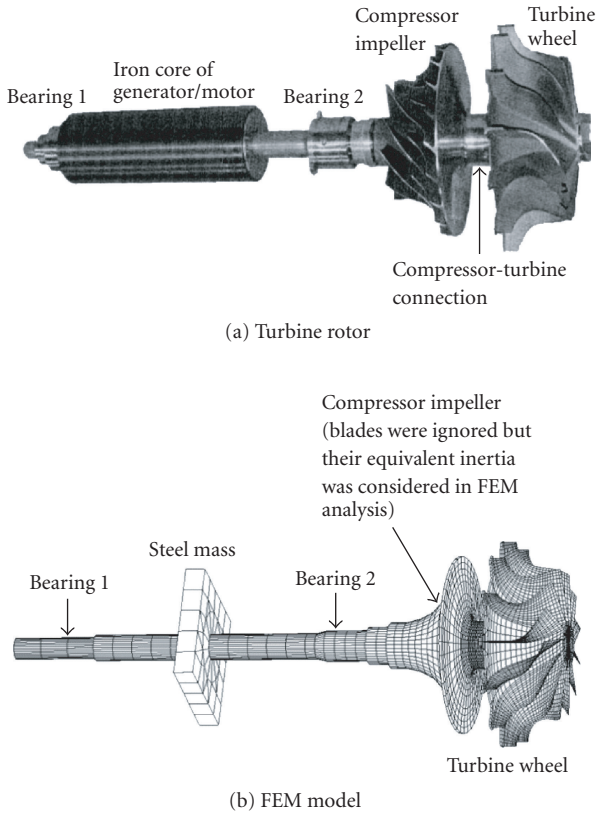

Figure 5: The turbine rotor and its FEM model.

is not significant. It is noted that Young's modulus identified in this research is the dynamic one. Dynamic modulus at high temperature may be larger than the static modulus at the same temperature since it is an adiabatic process in the dynamic test, while it is an isothermal process in static test [12].

3. VIBRATION MODES AND NATURAL FREQUENCIES OF TURBINE WHEEL

3.1. FEM analysis

Figure 5 shows the turbine rotor and its FEM model. The rotor consists of a shaft, a turbine wheel, a compressor impeller, and an iron core. The turbine wheel has 13 blades. Since this research is focused not on the vibration of the compressor impeller but on the blade vibration of the turbine wheel, the blades of the compressor impeller were modeled as equivalent inertia to the impeller hub (disk) in the analysis. The iron core was replaced by a steel mass both in the model experiment and in the FEM analysis (also see Figure 9).

FEM analysis was first done on the model shown in Figure 5 at room temperature and in a nonrotating state ($N = 0$) to understand the vibration modes. Average value of

Table 1: Natural frequencies and description of all the elastic modes in the frequency range of 0–7000 Hz, at room temperature and in a nonrotating state ($N = 0$).

Mode	Natural frequency (Hz)	Description	Mode shape
1	FEM: 327.5	Torsional mode of the shaft	
2	FEM: 357.8	Lateral mode of the shaft	
3	FEM: 1029.5	Lateral mode of the shaft	
4	FEM: 1620.4	Lateral mode of the shaft	
5	FEM: 2267.6 Experiment: 2212	Blade-shaft (longitudinal) coupled mode: a coupled mode between the 1st blade bending mode and longitudinal vibration of the shaft, dominated by the longitudinal vibration	Figure 6(a)
6	FEM: 2438.9 Experiment: 2385	Blade-shaft (torsional) coupled mode: a coupled mode between the 1st blade bending mode and the torsional vibration of the compressor-turbine connection	Figure 6(b)
7	FEM: 2554.9–2602.0 Experiment: 2400–2588	Blade-hub (disk) coupled mode: a coupled mode between the 1st blade bending mode and nodal diameter vibration of the hub (disk), dominated by the 1st blade bending mode	Figure 6(c)
8	FEM: 2809.4 Experiment: 2796	Blade-shaft (torsional) coupled mode: a coupled mode between the 1st blade bending mode and the torsional vibration of the compressor-turbine connection	Figure 6(d)
9	FEM: 3983.7	Lateral mode of the shaft	
10	FEM: 5191.8	Lateral mode of the shaft	
11	FEM: 6486.3–6531.0 Experiment: 6413–6713	Blade-hub (disk) coupled mode: a coupled mode between the 2nd blade bending mode and nodal diameter vibration of the hub (disk), dominated by the 2nd blade bending mode	Figure 6(e)
12	FEM: 6709.0 Experiment: 6613	Coupled mode between the 2nd blade bending mode and torsional vibration of the hub (disk)	Figure 6(f)

Young's modulus identified from all the specimens was used and Poisson's ratio was assumed to be 0.3 in the analysis. As for the boundary conditions, since the rotor was supported by two radial bearings in the model experiment (see Figure 9), only the radial (lateral) freedom at the locations of the two bearings was clamped. The axial freedom and the rotating freedom were set free, that is, the rotor can rotate and move in the axial direction freely and two rigid modes exist. The modes obtained in the frequency range of 0–7000 Hz, excluding the rigid ones, are listed in Table 1. Modes 1–4 and 9–10 are the torsional and lateral vibrations of the shaft. Modes 5–8 and 11–12 are the coupled blade bending modes which are shown in Figure 6. Blade vibration may be coupled with the torsional vibration and the longitudinal vibration of the shaft. It may also be coupled with the nodal diameter vibration of the hub (disk). Mode 5 in Figure 6 is a blade-shaft (longitudinal) coupled mode (a coupled mode between the 1st blade bending mode and the longitudinal vibration of the shaft). This mode is subject to the longitudinal vibration. Mode 6 and mode 8 are blade-shaft (torsional) coupled modes (coupled modes between the 1st blade bending mode and the torsional vibration of the shaft). The two modes are both strongly related with the torsion of the compressor-turbine connection (see Figure 5). The blades vibrate in the same direction circumferentially (same phase) as the hub (disk) in mode 6, but in the opposite direction (opposite phase) in mode 8. Mode 7 is a blade-hub (disk) coupled mode (a coupled mode between the 1st blade bending mode and the nodal diameter vibration of the hub (disk)). The coupling with different nodal diameters gives different natural frequencies. That is why a frequency band is indicated in the case of mode 7 (see Table 1). Physically, this mode consists of many different modes (the modes coupled with different nodal diameters). The frequency band is very narrow (limited) because the coupling is slight and the natural frequencies are mainly determined by the 1st blade bending mode. The fact that both the stiffness and the mass of the hub (disk) are quite larger than those of a blade makes the coupling slight. It was confirmed that vibration of this mode can be analyzed approximately by ignoring the hub (disk), that is, by applying a "clamped" boundary condition to the blade root. The same is mode 11, which is also a blade-hub (disk) coupled mode (a coupled mode between the 2nd blade bending mode and the nodal diameter vibration of the hub (disk)). Mode 12 is a coupled mode between the 2nd blade bending mode and the torsional vibration of the hub (disk).

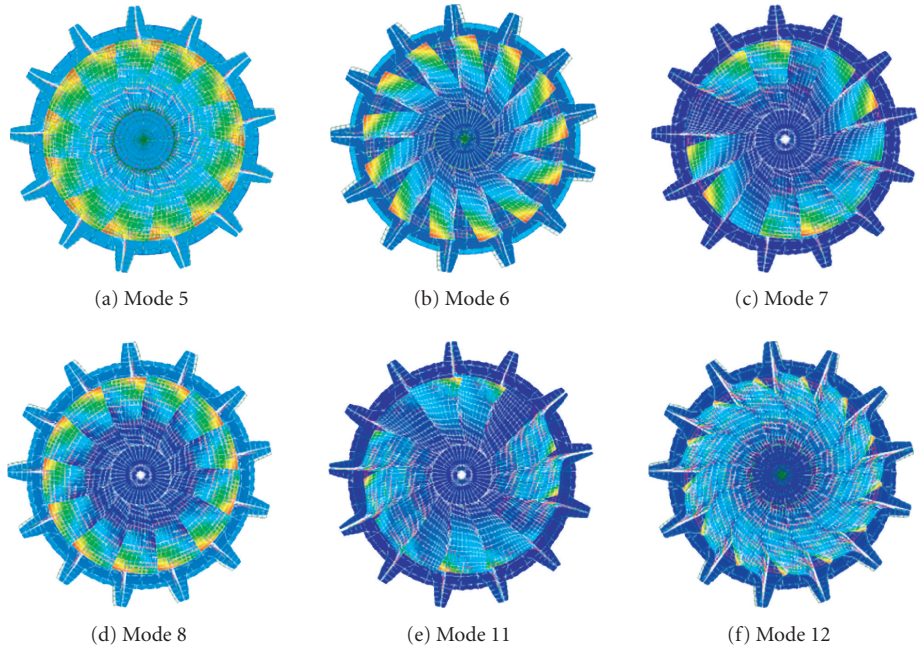

Figure 6: Blade bending modes of the turbine rotor shown in Figure 5.

Turbine blades work under a large centrifugal load at high temperature. The centrifugal load has an effect to increase the natural frequencies, while the high temperature decreases them. FEM analysis was done considering such effects. Since Young's modulus depends on temperature, what we were interested in was whether it is necessary to consider the temperature gradient (distribution of Young's modulus) from the leading edge to the trailing edge of a blade in vibration analysis. A pie slice model was used to analyze the vibration of a single blade. Based on CFD results [13] and thermal transfer analysis, it was assumed that, at the rated rotating speed, the metal temperature at the leading edge is 750°C and that at the trailing edge is 600°C. It was also assumed that the metal temperature in a nonrotating state ($N = 0$) is room temperature. Campbell's diagram obtained is shown in Figure 7 in which the solid lines indicate the results by considering the temperature gradient; the dashed lines, the results by using Young's modulus at the mean temperature from the leading edge to the trailing edge. The difference between the solid lines and the broken ones is slight. This indicates that temperature gradient is not an important factor, and applying the mean temperature is enough in vibration analysis. This conclusion is dependent on material and temperature. If the temperature gradient is much larger or the material is more sensitive to temperature, it may be necessary to consider the gradient. The three natural frequencies shown in Figure 7 are those of the bending modes of a single blade, not the coupled ones.

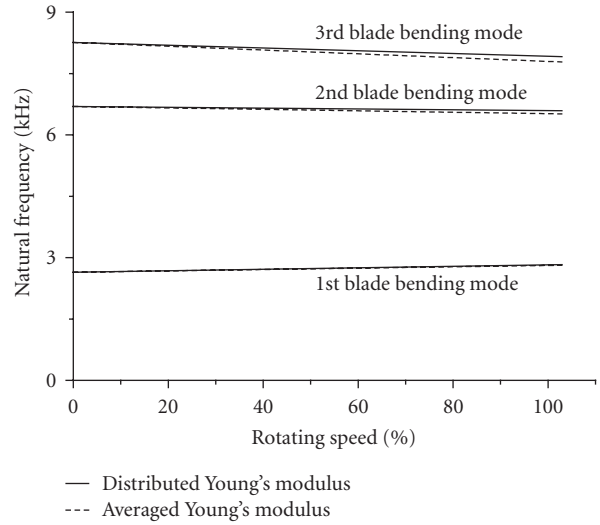

Figure 7: Campbell's diagram of the three lowest bending modes of a blade, considering both centrifugal effect and temperature effect (100% in the horizontal axis means the rated rotating speed).

3.2. Model experiment

Firstly, a small piezoelectric element was attached to a blade and harmonic voltage was applied to excite blade vibration. The modes measured by a laser holography system are shown in Figure 8. These are the blade bending modes coupled with the hub (disk), not the ones coupled with the shaft because excitations acting on a blade cannot excite blade-shaft coupled vibrations (see Section 4). The natural frequencies of the 1st blade bending mode and those of the 2nd one are given in Table 1 to compare with the FEM analysis (mode 7 and mode 11). Modal damping ratios were estimated from the frequency responses and they were found to be around 0.05%

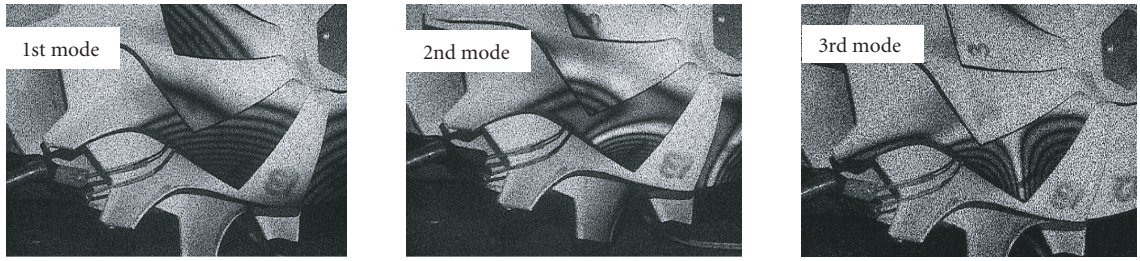

Figure 8: Blade bending modes measured by laser holography.

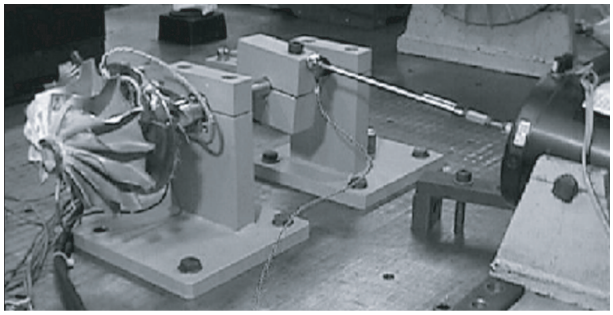

Figure 9: Setup of the model experiment for measuring blade stress excited by torsional excitations.

for all of the three lowest blade bending modes at room temperature. This value has the same order of the damping ratios measured on a turbine wheel during operation, by Iwaki et al. [8, 9].

Secondly, since the turbine wheel and the iron core of the generator/motor are connected directly by the same shaft, blade vibration may be excited by torque fluctuations. A model experiment was done at room temperature and in a nonrotating state ($N = 0$) to investigate which modes are more likely to be excited by torque fluctuations. Figure 9 shows the setup of the experiment, in which the iron core was replaced by a steel mass and a force was applied to the mass by a stinger to give a torsional excitation to the rotor. The stinger was driven by an exciter and the excitation force to the steel mass was measured by a load cell. This force applies a lateral excitation to the rotor at the same time. Since the natural frequencies of the coupled blade bending modes are quite different from those of the shaft's lateral modes, the lateral excitation did not excite blade vibration. Natural frequencies of the 1st blade bending mode, coupled with the shaft or the hub (disk), are in the range of 2212–2796 Hz, and those of the 2nd one are in the range of 6413–6613 Hz, while natural frequencies of the shaft's lateral modes are quite away from the two frequency ranges (see Table 1).

The vibration was measured by strain gauges and a laser holography system when the excitation frequency was swept from 2000 Hz to 7000 Hz slowly. The strain gauges were located at P1, P2, and P3 as shown in Figure 10. These points are the locations where the von Mises stress is the maximum for the three lowest bending modes of a blade (results by FEM analysis). The frequency spectrum of the stress at P1, excited by the torsional excitation, is plotted in Figure 11. The result by FEM is also plotted in the same graph for confirmation. Two peaks (peak A and peak B) can be observed in the frequency spectrum. This is the same for the stresses at both P2 and P3. Dominant frequencies of the two peaks are given in Table 1 (mode 6 and mode 8). The corresponding mode shapes measured by laser holography are shown in Figure 12. The two modes are the blade-shaft (torsional) coupled modes: mode 6 and mode 8, respectively (see Table 1 and Figure 6). Other modes were not observed.

4. DISCUSSIONS ON BLADE VIBRATION UNDER VARIOUS EXCITATIONS

4.1. Torque fluctuations

Figures 11 and 12 demonstrate that torque fluctuations can only excite resonance of the blade-shaft (torsional) coupled modes: mode 6 and mode 8 (see Table 1 and Figure 6). The blade-hub (disk) coupled modes are not excited. It is noted that mode 6 and mode 8 are strongly related with (dominated by) the torsion of the compressor-turbine connection (see Figure 5). It seems worthwhile to investigate what will occur if the natural frequency of a blade-shaft (torsional) coupled mode is close to that of the 1st bending mode of a blade. FEM analysis was done. Rotating inertia of the compressor impeller was changed in the analysis to move the natural frequencies of the blade-shaft (torsional) coupled modes. Changing the torsional stiffness of the compressor-turbine connection could achieve the same purpose. The blade stress at resonance of mode 6, excited by the torsional excitation acting on the steel mass as shown in Figure 9, was analyzed for different natural frequencies. The results are plotted in Figure 13, in which the horizontal axis represents the natural frequency of mode 6; the vertical axis and the amplitude of the stress at resonance (when the frequency of the torsional excitation coincides with the natural frequency of mode 6). Figure 13 shows that blade stress is large when the natural frequency of mode 6 is around 2500 Hz, which is close to the natural frequency of the 1st bending mode of a blade.

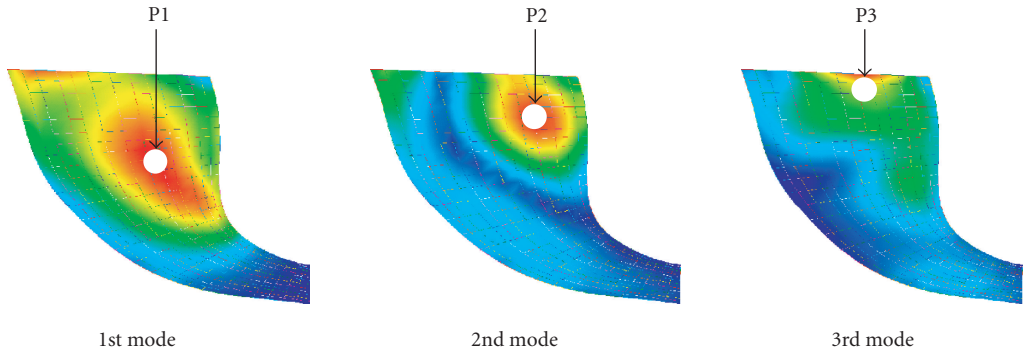

Figure 10: Locations of strain gauges (positions where the von Mises stress is the maximum for the three lowest blade bending modes).

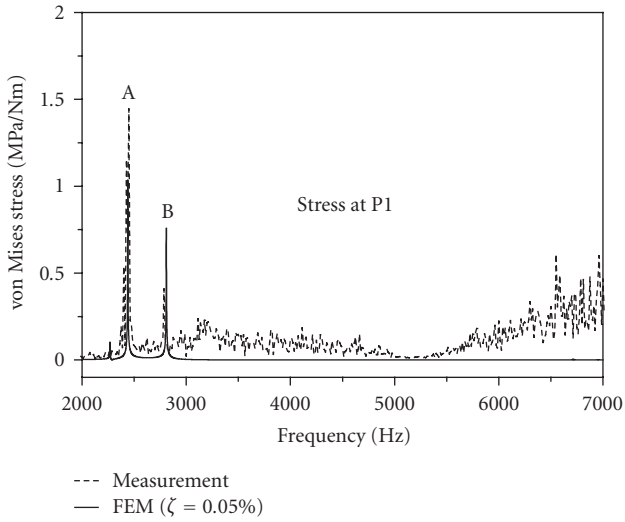

Figure 11: Blade stress excited by torsional excitation.

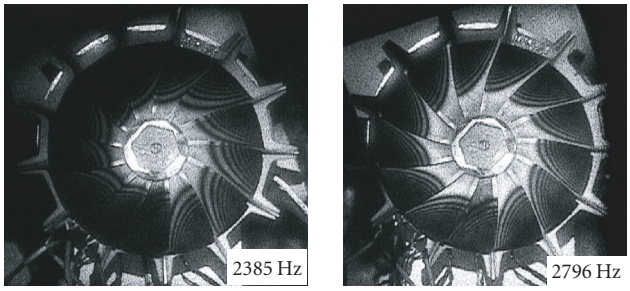

(a) Peak A in Figure 11 (b) Peak B in Figure 11

Figure 12: Modes of the turbine wheel excited by torsional excitation.

4.2. Impact excitations

To study the blade stress excited by impact excitations, a blade was excited by a mini impact hammer at a point shown in Figure 14 and the response (stress) was measured by strain gauges. The stress at P1 is given in Figure 15 in which the result by FEM is also plotted for confirmation. Peak C and peak D in Figure 15 correspond to the blade-hub (disk) coupled modes: mode 7 and mode 11, respectively (see Table 1 and Figure 6). Mode 7 is the coupled vibration between the 1st blade bending mode and the hub (disk). Mode 11 is the coupled vibration between the 2nd blade bending mode and the hub (disk). Figure 15 demonstrates that only the blade-hub (disk) coupled modes are excited by impact excitations. This is because the mass of a blade is much smaller than that of the whole rotor.

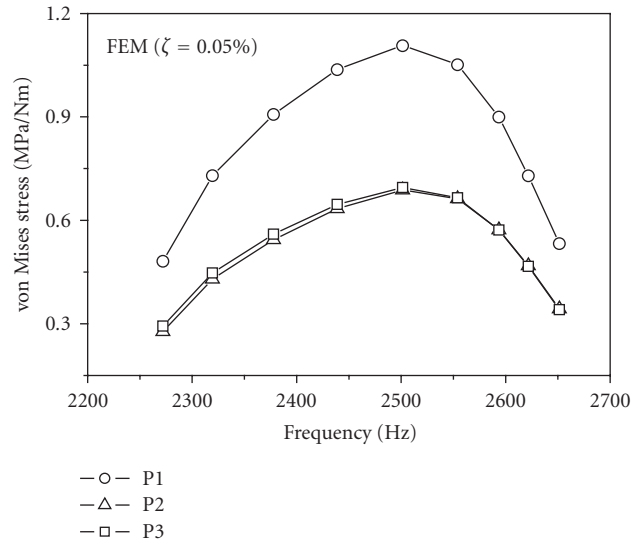

Figure 13: Blade stress at resonance versus natural frequency of mode 6 (FEM analysis) (see Table 1 and Figure 6 for mode 6).

4.3. Pressure fluctuations

The turbine investigated in this research is an annular type. Hot gas is guided to the turbine wheel by nozzle vanes. A typical excitation source is rotor-stator interaction (the interaction between the turbine blades and the vanes). It features dominant frequencies of ZnN and its higher harmonics. An annular turbine usually has many nozzle vanes and ZnN is

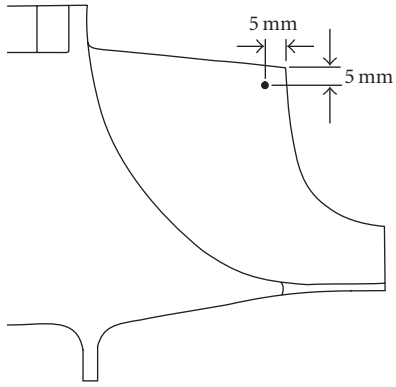

Figure 14: Excitation point by a mini impact hammer.

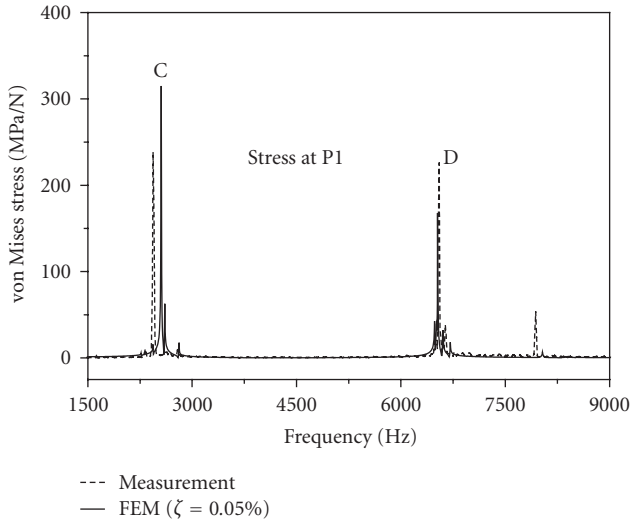

Figure 15: Blade stress excited by an impact excitation.

much higher than the natural frequencies of the lower blade bending modes, no matter which mode is coupled with the hub (disk) or the shaft. So, ZnN and its higher harmonics are not destructive. It is the N and its higher harmonics that should be considered carefully in design. The pressure fluctuations of N and its higher harmonics may be caused by circumferential unevenness of hot gas, eccentricity between the turbine wheel and nozzle vanes, dimensional scatters of blades and vanes, and so forth. It is difficult to predict the pressure fluctuations quantitatively. Designers usually separate the lower natural frequencies from the higher harmonics of N by optimizing blade profile and thickness to prevent resonance, and consider a specific alternating stress, say 10% of the static stress under centrifugal, thermal, and pressure loads, to evaluate high cycle fatigue.

In this research, to understand which mode is more likely to be excited, the responses under certain pressure excitations were analyzed. Although there is no information about how the fluctuations of the N and its higher harmonic components act on the blades, considering that they may be uneven circumferentially, and also, they may propagate circumferentially as the fluctuations induced by rotor-stator interaction, three cases were analyzed. They are (1) the fluctuations act onto all the 13 blades simultaneously in the same phase (uniform pressure fluctuations); (2) the fluctuations act onto only one blade; (3) the fluctuations propagate circumferentially around the turbine wheel (propagating pressure fluctuations). The propagating speed from the view of the rotating turbine wheel was assumed to be the same as the rotation but in the opposite direction, that is, the fluctuations are stationary from the view of the casing. Based on CFD analysis and experience, it was assumed that the pressure fluctuation over a blade has the same distribution with the blade steady pressure and that the amplitude, which is the location dependent over a blade, is 1% of the steady pressure at design point in all the three cases. In the case of propagating fluctuations, the fluctuations were applied to the blades with different phases. The phase difference between two adjacent blades is $2\pi/13$ (the turbine wheel has 13 blades), that is, the fluctuations were applied to the blades as a traveling wave propagating around the turbine wheel. This kind of propagating fluctuations is usually observed in rotor-stator interaction. The steady pressure was obtained by CFD using the commercial Navier-Stokes solver TASCflow [13]. The value of 1% is the same order as the fluctuations induced by rotor-stator interaction (ZnN component), which was analyzed by unsteady CFD using the same solver.

As the results of FEM analysis, the frequency responses of the stress at P1 are shown in Figure 16, in which peaks A and B correspond to the blade-shaft (torsional) coupled modes (modes 6 and 8 in Table 1 and Figure 6); peaks C and D correspond to the blade-hub (disk) coupled modes (modes 7 and 11); peak E corresponds to the blade-shaft (longitudinal) coupled mode (mode 5); peak F corresponds to the 2nd blade bending mode which is coupled with the torsional vibration of the hub (disk) (mode 12).

Figure 16 demonstrates that if the pressure fluctuations act onto all the blades simultaneously in the same phase, only the blade-shaft (torsional, longitudinal) coupled modes and the 2nd blade bending mode coupled with the torsional vibration of the hub (disk) are excited. If they act onto one blade, or if they propagate circumferentially, only the blade-hub (disk) coupled modes are excited.

5. CONCLUSIONS

Young's modulus of the blades of a real radial inflow micro gas turbine wheel was investigated to understand its dependence on temperature, its scattering, and the possible existence of anisotropy. It was demonstrated that Young's modulus decreases as temperature increases and this temperature dependence should be considered in vibration analysis. Anisotropy and scattering were not significant even at high temperature. As for the influence of temperature gradient (distribution of Young's modulus) from the leading edge to the trailing edge of a blade, it was confirmed that the temperature gradient can be ignored by applying the mean temperature in vibration analysis.

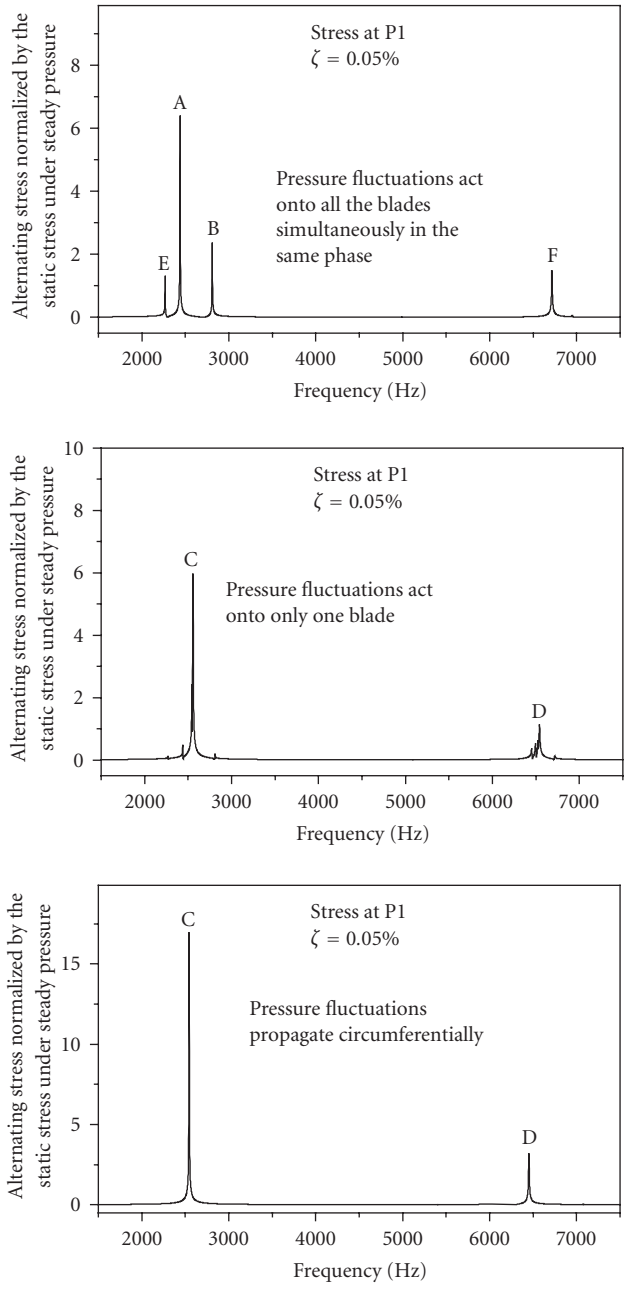

Figure 16: Responses under different pressure excitations (FEM analysis).

Turbine blades suffer many excitations during operation. Meanwhile, they have many kinds of vibration modes. Model experiments and FEM analysis were conducted to identify the modes which are more likely to be excited. Torque fluctuations, impact excitations as well as pressure fluctuations were discussed. It was demonstrated that torque fluctuations and uniform pressure fluctuations (fluctuations acting on all the blades simultaneously in the same phase) are more likely to excite resonance of blade-shaft (torsional, longitudinal) coupled modes, and the vibration is large when the natural frequency of a blade-shaft (torsional) coupled mode is close to that of the 1st bending mode of a blade. On the other hand, impact excitations and propagating pressure fluctuations (fluctuations propagating circumferentially around the turbine wheel) are more likely to excite resonance of blade-hub (disk) coupled modes.

NOMENCLATURE

Zn: Number of nozzles
N: Rotating frequency of the turbine wheel
ζ: Modal damping ratio.

ACKNOWLEDGMENTS

The author would like to thank Professor Sakata and Mr. Matsui of Takushyoku University for their cooperation and invaluable advices, especially in regard to the measurement of natural frequencies at high temperature. The author would also like to thank Dr. Dewis of EESI (Elliott Energy Systems Inc.) for his invaluable discussions and professional opinions. The work was done when the author was working with Ebara Research Co., Ltd.

REFERENCES

[1] D. T. Hooie, "High efficiency engines and turbines: pathway to a sustainable, clean energy future," in *International Symposium on Distributed Energy Systems in the 21st Century*, Tokyo, Japan, September 2002.

[2] T. W. Simon and N. Jiang, "Development and applications of microturbines," in *International Symposium on Distributed Energy Systems in the 21st Century*, Tokyo, Japan, September 2002.

[3] P. P. Walsh and P. Fletcher, *Gas Turbine Performance*, Blackwell Science, Malden, Mass, USA; ASME, New York, NY, USA, 1998.

[4] M. S. Y. Ebaid, F. S. Bhinder, and G. H. Khdairi, "A unified approach for designing a radial flow gas turbine," *Journal of Turbomachinery*, vol. 125, no. 3, pp. 598–606, 2003.

[5] *Aerospace Structural Metals hand book*, versions of 1976, 1999, and 2001.

[6] H.-A. Kuhn and H.-G. Sockel, "Elastic properties of textured and directionally solidified nickel-based superalloys between 25 and 1200°C," *Materials Science and Engineering A*, vol. 112, no. 1-2, pp. 117–126, 1989.

[7] T. Kreuz-Ihli, D. Filsinger, A. Schulz, and S. Wittig, "Numerical and experimental study of unsteady flow field and vibration in radial inflow turbines," *Journal of Turbomachinery*, vol. 122, no. 2, pp. 247–254, 2000.

[8] F. Iwaki, K. Mitsubori, H. Taguchi, C. Chino, and Y. Hirata, "Strength evaluation to develop the high pressure turbocharger (1st report, evaluation of the blade vibration)," *Journal of the Gas Turbine Society of Japan*, vol. 29, no. 3, pp. 188–193, 2001 (Japanese).

[9] F. Iwaki, K. Mitsubori, H. Taguchi, C. Chino, and M. Obata, "Strength evaluation to develop the high pressure turbocharger (2nd report, influence of turbine scroll on blade vibration)," *Journal of the Gas Turbine Society of Japan*, vol. 29, no. 6, pp. 493–497, 2001 (Japanese).

[10] M. Sakata, K. Kimura, and J. Shimojo, "Measurement of isotropic and anisotropic elastic moduli from the impact sound

of engineering ceramics and composites at elevated temperatures," in *International Symposium on Impact Engineering*, I. Maekawa, Ed., vol. 2, pp. 502–507, Sendai, Japan, November 1992.

[11] M. Sakata and H. Ohnabe, "Measurement of elastic moduli from the impact sound of ceramic matrix composites at elevated temperatures," in *Proceedings of the 9th Technical Conference of the American Society for Composites*, pp. 79–86, Newark, Del, USA, September 1994.

[12] L. W. Sink, G. S. Hoppin III, and M. Fujii, "Low-cost directionally-solidified turbine blades," Tech. Rep. NASA-CR-159464, AirResearch-21-2953-1, pp. 243–247, NASA, Washington, DC, USA, January 1979.

[13] H. Watanabe, M. Zangeneh, H. Okamoto, S. Guo, and A. Goto, "Optimization of microturbine aerodynamics using CFD, inverse design and FEM structural analysis (2nd report: turbine design)," in *Proceedings of the ASME Turbo Expo*, pp. 1545–1552, Vienna, Austria, June 2004, GT2004-53583.